Monthly Notices of the ROYAL ASTRONOMICAL SOCIETY
MNRAS **548**, 1–6 (2026)
Advance Access publication 2026 March 27
https://doi.org/10.1093/mnras/stag570

A potential meteorite-producing Taurid fireball observed in 2021

José M. Madiedo[1,2*]
[1] *Facultad de Ciencias Experimentales, Universidad de Huelva, E-21071 Huelva, Spain*
[2] *Instituto de Astrofísica de Andalucía, CSIC, Apt. 3004, Camino Bajo de Huetor 50, E-18080 Granada, Spain*

Accepted 2026 March 17. Received 2026 March 13; in original form 2025 November 30

ABSTRACT

On 2021 November 12, a Taurid fireball with an absolute magnitude of −13 was recorded over Spain. This work presents the analysis of this impressive bolide, which penetrated the atmosphere till a remarkable low final height of about 25.1 km above the ground level. A non-zero mass was calculated at the ending point of the luminous trajectory, which means that this event would have produced a meteorite that fell on the ground. Despite the mass of the fragment being small, of around 6.5 g, this would confirm the possibility of Taurid meteorite survival, a debate that was initiated some years ago. The emission spectrum of this fireball is also discussed.

Key words: meteorites, meteors, meteoroids.

1. INTRODUCTION

Different names are assigned to different parts of the Taurid meteoroid complex, which in addition are divided into North and South branches (P. B. Babadzhanov & I. V. Obrubov 1991; P. Jenniskens 2006, 2023): the Piscids, the Arietids, the Taurids, and the χ-Orionids. It has been proposed that this complex includes a swarm of meteoroids trapped in the 7:2 resonance with Jupiter, which could account for enhanced activity of bright Taurid fireballs in certain years (D. J. Asher & S. V. M. Clube 1993). The predictions based on this hypothesis were able to anticipate an activity increase of Taurid bolides in 2015, and a new branch of the Taurids was identified during the monitoring of this stream that year (P. Spurny et al. 2017; H. A. R. Devillepoix et al. 2019).

It has been established that this meteoroid complex is associated with Comet 2P/Encke (F. L. Whipple 1940). Several authors have proposed that this comet, along with a large number of near-Earth objects (NEOs), constitutes a remnant of the cascade fragmentation of a giant comet approximately 40 km in diameter. This disintegration process may have occurred around 20 000 yr ago and is also believed to have given rise to the Taurid meteoroid complex. (V. Clube & W. Napier 1982; D. J. Asher 1991; D. I. Steel et al. 1991; D. J. Asher et al. 1993; D. I. Steel & D. J. Asher 1996). However, several authors have argued that the parent comet was much smaller (e.g. P. Jenniskens 2006).

The capability of meteoroids from major meteor showers to produce meteorites has been a longstanding topic of debate. It is well established that even metre-sized, friable cometary meteoroids are typically destroyed at high altitudes in the atmosphere (e.g. Z. Ceplecha 1988). However, materials with high tensile strength have also been identified within cometary streams, as well as in sporadic meteoroids associated with Halley-type comet and Jupiter-family comet orbits (N. A. Konovalova 2003). These more robust meteoroids can produce deep-penetrating bolides (see e.g. J. M. Madiedo et al. 2014), although their high pre-atmospheric velocities significantly reduce the likelihood of meteorite survival (Z. Ceplecha et al. 1998).

Meteorite survival is therefore more plausible for stronger particles originating from low-velocity streams: the lower the pre-atmospheric velocity and the greater the material strength, the higher the probability of surviving atmospheric entry. Additionally, shallow entry angles further increase this likelihood. Within this framework, the Taurid stream has been suggested as a potential source of meteorites (P. Brown et al. 2013; J. M. Madiedo et al. 2014). The stream is known to contain large meteoroids – up to metre-sized (G. W. Wetherill 1974) – and exhibits relatively moderate entry velocities in the atmosphere ($\sim$28 km s^{-1}). Moreover, some Taurid meteoroids have been found to possess exceptionally high mechanical strength (N. A. Konovalova 2003), further enhancing their potential to produce meteorites. It is worth mentioning that both Sutter's Mill and Maribo CM carbonaceous chondrites are examples of recovered meteorites associated with fireballs with entry speeds of $\sim$28 km s^{-1} (H. Haack et al. 2012; P. Jenniskens et al. 2012).

This hypothesis was investigated by P. Brown et al. (2013) through the analysis of a deep-penetrating Taurid bolide observed over Canada in 2010, for which a terminal mass below 10 g was estimated. Based on this event, they proposed a limiting velocity for meteorite survival of approximately 29 km s^{-1}. However, evidence was presented supporting the ability of Geminid meteoroids (despite their higher entry velocity of $\sim$35 km s^{-1}) to generate meteorite-dropping events (J. M. Madiedo et al. 2013). This result suggests that the velocity threshold proposed by P. Brown et al. (2013) may have been underestimated, implying that the potential for Taurid meteoroids to survive atmospheric

* Email: madiedo@meteoroides.net

Table 1. Geographical coordinates of the SWEMN meteor-observing stations that participated in this work.

Station #	Station name	Longitude (W)	Latitude (N)	Alt. (m)
1	La Hita	3°11′00″	39°34′06″	674
2	El Guijo	4°01′53″	40°36′27″	907

entry and produce meteorites could be greater than previously assumed.

The systematic monitoring of bright meteors during the Taurid activity period is essential for identifying those events that may be potential meteorite-producing candidates. This monitoring is being performed in Spain by means of high sensitivity cameras in the framework of the SMART project (J. M. Madiedo 2014), which also employs a set of spectrographs to investigate the chemical composition of the associated meteoroids. The SMART survey started operation in 2006 and is currently being conducted by the Southwestern Europe Meteor Network (SWEMN; J. M. Madiedo et al. 2021). This work analyses a deep-penetrating Taurid fireball observed on 2021 November 12. This is, in fact, the Taurid meteor event with the lowest terminal point recorded by the SMART survey to date. Besides, a non-zero terminal mass was inferred from the analysis of its atmospheric path, which would confirm the ability of the Taurids to produce meteorites. The emission spectrum of this event is also analysed and discussed.

2. INSTRUMENTATION AND METHODS

The fireball discussed in this work was recorded from two meteor-observing stations operated by the SMART survey in Spain. Their geographical positions are listed in Table 1. These meteor stations employed a set of low-lux CCD video cameras manufactured by Watec Corporation (models 902H2 and 902H2 Ultimate). The field of view of these devices ranges from 62 × 50° to 14 × 11°. A detailed description about these systems and their operation is given in previous papers (see, for instance, J. M. Madiedo 2014, 2017). In order to obtain information about the chemical nature of meteoroids ablating in our atmosphere, some of these CCD cameras are configured as video spectrographs (J. M. Madiedo 2015a, b). For this purpose, holographic diffraction gratings (500 or 1000 lines mm^{-1}, depending on the device) are attached to their objective lens.

As in previous works, the technique described in J. M. Madiedo (2015a, b) has been followed for data reduction. Thus, the position of the meteor was measured by hand in the video frames acquired by the CCD cameras. In this way, the plate (x, y) coordinates of the fireball along its apparent path from each meteor station were obtained. These values were then converted into equatorial coordinates by the SAMIA software (J. M. Madiedo et al. 2021) by using the position of reference stars appearing in the images. This software employs the method of the intersection of planes to calculate the coordinates of the apparent radiant and also to infer the atmospheric path of the fireball (Z. Ceplecha 1987). The heliocentric orbit followed by the parent meteoroid before its encounter with our planet was obtained by following the standard technique described in Z. Ceplecha (1987).

The emission spectrum of the fireball was captured by means of a CCD video spectrograph operating at La Hita astronomical observatory (observing station number 1 in Table 1). This spectrum was analysed with the CHIMET software, which follows the standard procedure described in J. M. Madiedo (2017). In this way, the interlaced video file containing this signal was first deinterlaced. Next, each resulting deinterlaced video frame was sky-background-subtracted and flat-fielded. Since the high luminosity of the fireball gave rise to saturation in the frames corresponding to the phase of maximum brightness of the event, we only considered those video frames where the spectral lines were not saturated, and assumed that these would represent the bulk composition of the parent meteoroid. The spectrum was then calibrated in wavelengths by identifying typical lines found in meteor spectra, such as those of neutral Na, Mg, and Ca. Finally, the calibrated spectrum was corrected by taking into account the instrumental efficiency of the recording device. To obtain information about the chemical nature of the meteoroid, the contributions of Mg I-2, Na I-I, and Fe I-15 multiplets were measured in the fireball spectrum, frame by frame. Then, the contributions in each video frame were added to obtain the integrated intensity of the above-mentioned multiplets along the atmospheric path of the bolide.

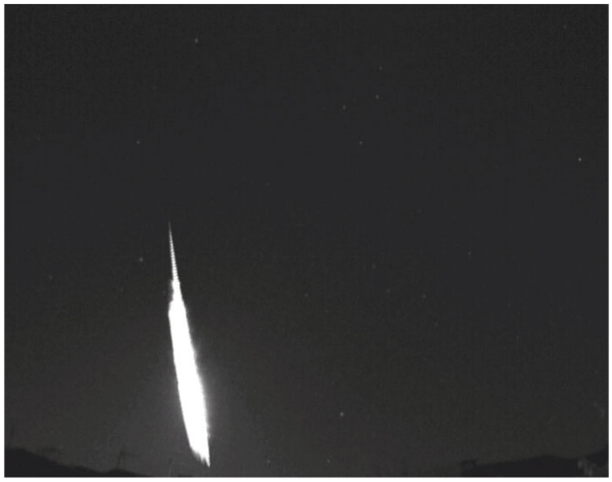

Figure 1. Sum-pixel image of the SWEMN20211112_003 448 meteor event recorded from El Guijo observatory.

3. OBSERVATIONS

On 2021 November 12, at $0^h34^m48.0 \pm 0\overset{s}{.}1$ UT, three video cameras operating in the framework of the SMART project recorded a bright fireball (Fig. 1). Two of these cameras were located at the position labelled as 1 (La Hita) in Table 1, and the third device was located at El Guijo (position 2 in Table 1). The bolide was included in the SWEMN data base under the code SWEMN20211112_003448. The peak luminosity of this event corresponded to an absolute magnitude of −13.0 ± 0.5, and the bolide lasted around 3.2 s. The analysis of its atmospheric path revealed that the luminous phase began at an altitude of 96.7 ± 0.4 km above sea level, and ended at a remarkable low height of 25.1 ± 0.5 km. In total, the distance travelled by the fireball in the atmosphere was around 77 km. As shown in Fig. 2, this trajectory was located over the province of Salamanca (north of Spain). Our analysis reveals that the progenitor meteoroid hit the Earth's atmosphere with a velocity $V_\infty = 27.9 \pm 0.3$ km s^{-1}, with the apparent radiant of the meteor located at the coordinates $\alpha = 56.81 \pm 0.08°$, $\delta = 16.12 \pm 0.07°$. The calculation of the geocentric radiant (J2000) yields $\alpha_g = 55.39 \pm 0.08°$, $\delta_g = 14.93 \pm$

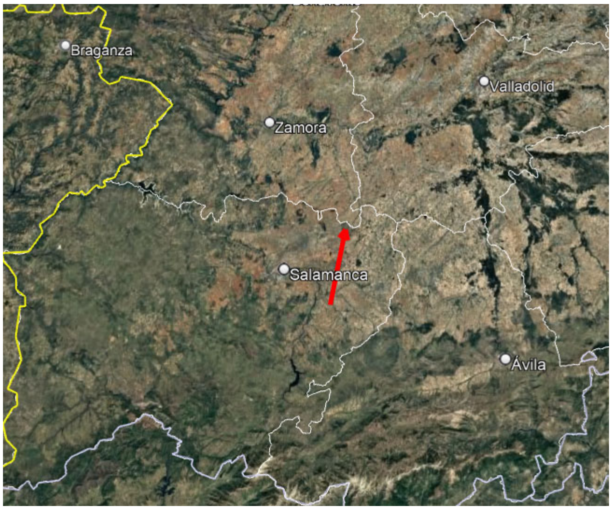

Figure 2. Projection on the ground of the atmospheric path of the SWEMN20211112_003 448 fireball.

0.07°. These trajectory and radiant parameters are summarized in Table 2. The parameters that define the heliocentric orbit of the meteoroid before its encounter with our planet are listed in Table 3, where a is the semimajor axis, e the orbital eccentricity, i the orbit inclination, ω the argument of perihelion, Ω the longitude of the ascending node, and q the perihelion distance. To confirm the association of the meteoroid with the Southern Taurid stream we have employed the Southworth & Hawkins D_{SH} dissimilarity function (R. B. Southworth & G. S. Hawkins 1963). Thus, the D_{SH} value obtained by comparing the orbit of this stream (P. Jenniskens et al. 2016) with the orbit of the meteoroid yields $D_{SH} = 0.05$, which is lower than the 0.15 cut-off value usually taken to establish a valid association (B. A. Lindblad 1971a, b). Nevertheless, some NEOs evolving from the $\nu6$ secular resonance may exhibit orbital parameters similar to those of the Southern Taurids. This resonance is caused by the s-Taurid stream, and it can be a likely source of LL or L meteorites (P. Jenniskens & H. A. R. Devillepoix 2025). By comparing the orbit of the s-Taurid stream (P. Jenniskens et al. 2016) with the orbit of the meteoroid, the D_{SH} dissimilarity function yields $D_{SH} = 0.13$, which is also below the above-mentioned cut-off value, but larger than the value obtained for the Southern Taurids. However, the calculated position of the geocentric radiant of the s-Taurids, once corrected by taking into account the radiant drift, yields $\alpha_g = 61.20^\circ$, $\delta_g = 16.21^\circ$, which differs significantly from the calculated geocentric radiant of the bolide. For this reason it was considered that this meteor probably did not belong to the s-Taurids.

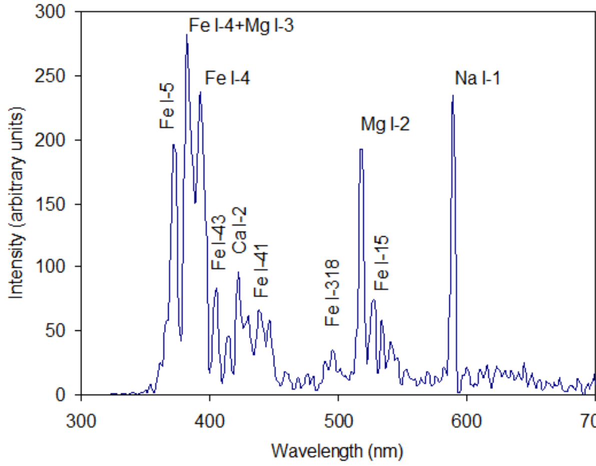

Figure 3. Emission spectrum of the SWEMN20211112_003 448 bolide. In this plot, intensity is expressed in arbitrary units.

The calibrated emission spectrum of the bolide is shown in Fig. 3. The main contributions have been labelled in this plot by following the multiplets notation given by C. E. Moore (1945). As usual in meteor spectra, most lines correspond to the emission associated to neutral Fe atoms. As can be noticed, the most significant lines from Fe I are those of Fe I-5 (373.7 nm), Fe I-4 (382.4 and 392.2 nm), Fe I-43 (404.5 nm), Fe I-41 (438.3 nm), and Fe I-15 (526.9 and 542.9 nm). The contribution from Mg I-3 at 382.9 nm is blended with that of Fe I-4 at 382.4 nm. The emissions from the Mg I-2 triplet at 516.7 nm and the Na I-1 doublet at 588.9 nm are also very remarkable, and the line of Ca I-2 (422.6 nm) was also identified. The resulting values for the Na/Mg and the Fe/Mg intensity ratios are Na/Mg = 1.21 and Fe/Mg = 0.89, respectively. According to fig. 5 in J. Borovička et al. (2005), this Na/Mg ratio fits fairly well the result expected for chondritic meteoroids when the meteor velocity is of about 28 km s^{-1}.

4. DISCUSSION

4.1. Photometric analysis

Fig. 43 shows the light curve obtained by measuring the luminosity of the fireball along its atmospheric trajectory. These photometric data were employed to derive the ablated meteoroid mass, by means of the classical mass–luminosity relationship:

$$m_p = 2 \int_{t_e}^{t_b} I_p / \left(\tau v^2\right) \mathrm{d}t. \quad (1)$$

Table 2. Trajectory and radiant data (J2000) of the SWEMN20211112_003 448 fireball. H_b and H_e: beginning and ending heights. α_g and δ_g: right ascension and declination of the geocentric radiant. V_∞ and V_g: observed pre-atmospheric and geocentric velocities.

H_b (km)	H_e (km)	α_g (°)	δ_g (°)	V_∞ (km s^{-1})	V_g (km s^{-1})
96.7 ± 0.4	25.1 ± 0.5	55.39 ± 0.08	14.93 ± 0.07	27.9 ± 0.3	25.6 ± 0.3

Table 3. Orbital parameters (J2000) of the progenitor meteoroid of the SWEMN20211112_003 448 fireball.

a (au)	e	i (°)	q (au)	ω (°)	Ω (°)
2.24 ± 0.08	0.799 ± 0.008	4.34 ± 0.08	0.449 ± 0.003	103.2 ± 0.1	49.51718 ± 10^{-5}

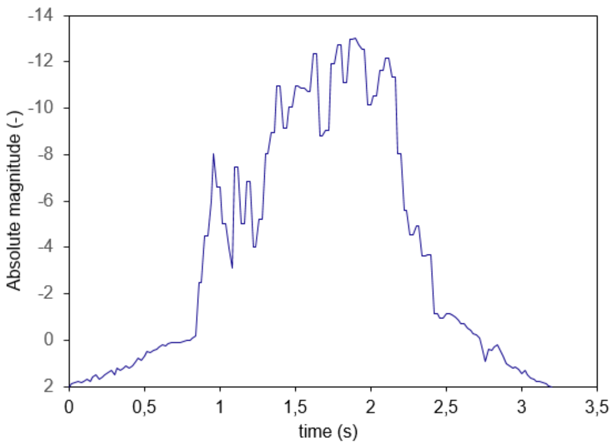

Figure 4. Light curve of the SWEMN20211112_003 448 fireball.

Here m_p is the meteoroid mass ablated during the luminous phase of the event, from its beginning time t_o till its ending time t_e. The luminosity of the meteor is I_p, which is related to the absolute magnitude M of the meteor by means of the following equation:

$$M = -2.5 \log(I_p/I_0), \quad (2)$$

where I_0 is the luminosity of a zero-magnitude star. For the calculation of the luminous efficiency (τ), the equations given by Z. Ceplecha & R. E. McCrosky (1976) were employed. From this analysis, the ablated mass yields $m_p = 16 \pm 2$ kg. By assuming a bulk density of 1.6 g cm^{-3} for Taurid meteoroids (P. B. Babadzhanov & G. I. Kokhirova 2009; P. Jenniskens 2023) and spherical shape, this mass would correspond to a meteoroid diameter of 27 ± 1 cm.

As can be noticed in Fig. 4, the maximum brightness of the event was reached 1.9 s after the beginning of its luminous phase. But 1 s before that stage it experienced a sudden increase in brightness, reaching an absolute magnitude of -8.0 ± 0.5. This remarkable increase in luminosity occurred as a consequence of the sudden disruption of the meteoroid when this particle was located at an altitude of 66.2 ± 0.5 km. By analysing the conditions at this point, the toughness of the particle can be evaluated, since this breakup takes place when the aerodynamic pressure exceeds the tensile strength of the meteoroid. The value of this aerodynamic pressure S is provided by the following equation (V. A. Bronshten 1981):

$$S = \rho_{atm} \cdot v^2. \quad (3)$$

Here v and ρ_{atm} are the velocity of the meteoroid and the density of air at the disruption point, respectively. The US Standard Atmosphere Model (U.S. Standard Atmosphere 1976) has been employed to obtain this air density.

In this way, it was obtained that the disruption of the meteoroid occurred under a dynamic pressure of 0.10 ± 0.01 MPa. Previous studies have revealed that Taurid meteoroids exhibit large variations in strength. For instance, according to N. A. Konovalova (2003) particles from this stream were found to exhibit fragmentation under aerodynamic pressures ranging from 0.05 to 0.18 MPa, while P. Matlovic et al. (2017) analysed Taurid events that exhibited a range comprised between 0.02 and 0.10 MPa. According to this, the meteoroid that gave rise to the fireball analysed here would belong to a population of tougher members in the stream. This could account for its extraordinary capability to penetrate the atmosphere till the calculated final altitude of 25.1 ± 0.5 km.

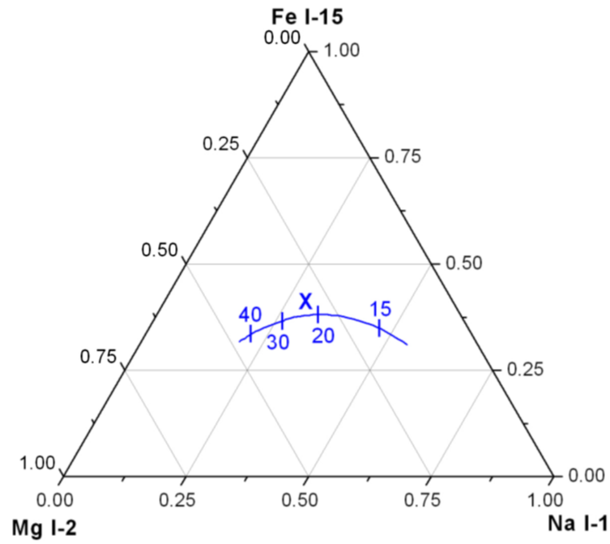

Figure 5. Expected relative intensity (solid line), as a function of meteor velocity (in km s^{-1}), of the Na I-1, Mg I-2, and Fe I-15 multiplets for chondritic meteoroids (J. Borovička et al. 2005). The cross shows the experimental relative intensity obtained for the fireball discussed here.

4.2. Emission spectrum

Information related to the likely nature of the progenitor meteoroid can be derived from the analysis of the relative intensity of the emission lines associated with multiplets Na I-1, Mg I-2, and Fe I-15 (J. Borovička et al. 2005). To confirm the likely chondritic nature of the parent meteoroid of the SWEMN20211112_003 448 event, the Na I-1, Mg I-2, and Fe I-15 relative intensities were plotted in a ternary diagram (Fig. 5). The solid line in this diagram corresponds to the relative intensity expected for chondritic meteoroids as a function of meteor velocity (J. Borovička et al. 2005). As can be seen, the value derived from the analysis of the fireball spectrum fits fairly well the theoretical relative intensity corresponding to chondritic meteoroids moving at velocity of about 28 km s^{-1}. This result agrees with previous results obtained from the emission spectrum of other Taurid fireballs (J. M. Madiedo et al. 2014; P. Matlovič et al. 2017). So, in addition to the low value found for the Southworth–Hawkins dissimilarity function ($D_{SH} = 0.05$), spectral evidence also supports the association of this meteoroid with the Taurid complex.

4.3. Dark flight and meteorite survival

Since the altitude of the terminal point of the luminous trajectory of the bolide was low and the tensile strength of the progenitor meteoroid was high, it was considered that the meteor event discussed here was a potential meteorite producer. The particle mass at this terminal point (m_E) was calculated by employing the following relationship (Z. Ceplecha et al. 1983):

$$m_E = \left(\frac{1.2 \rho_E v_E^2}{(dv/dt)_E \rho_m^{2/3}} \right). \quad (4)$$

Here the parameters V_E and $(dv/dt)_E$ are the velocity and the deceleration of the meteoroid at the terminal point of the luminous path of the event, respectively. These parameters were obtained from the analysis of the atmospheric trajectory of the fireball, and yield $v_E = 3.9 \pm 1.1$ km s^{-1} and $(dv/dt)_E = -9 \pm 3$ km s^{-2}. The bulk density of the meteoroid is ρ_m, which was assumed

Figure 6. Strewn field showing the position calculated for different masses. North is up.

to be $\rho_{\mathrm{m}} = 1.6\,\mathrm{g\,cm^{-3}}$ (P. B. Babadzhanov & G. I. Kokhirova 2009). ρ_{E} is the air density at the ending point of the fireball, which was estimated by means of the US standard atmosphere model (U.S. Standard Atmosphere 1976). With these values the terminal mass calculated from equation (4) is $m_{\mathrm{E}} = 6.5^{\{+15.5\}}_{\{-4.8\}}$ g.

To calculate the dark flight of the surviving mass it has been considered that this mass was not fragmented and that this single particle was spherical in shape. This dark phase of the atmospheric trajectory was modelled by employing the SAMIA software, which follows the standard procedure described by Z. Ceplecha (1987). To account for the influence of atmospheric conditions on these calculations the atmospheric data provided by AEMET (the Spanish meteorological agency) were employed. These calculations show that the meteorite fell at the geographical coordinates 41°.1097N, 5°.3117W. This position corresponds to an agricultural area located in the north-eastern part of the province of Salamanca (northern Spain). Fig. 6 shows the calculated strewn field. In this map, the position mark of the 6 g fragment corresponds to the above-mentioned geographical coordinates. Despite the small nominal value obtained for the surviving mass, an expedition was organized to the landing area, where experts in meteorite recovery participated in collaboration with the SWEMN network. But unfortunately it was found that most of part of the predicted area had just been plowed, and the meteorite was not found.

5. CONCLUSIONS

This work presents the analysis of a magnitude −13 fireball recorded over Spain on 2021 November 12. According to the radiant position and the orbital parameters derived from the analysis of the event, the meteoroid belonged to the southern branch of the Taurid stream. The path in the atmosphere of this bright meteor was also calculated. It was found that the luminous phase of the event ended at a height of about 25.1 km. The low altitude of this terminal point can be explained because of the high tensile strength found for the meteoroid: around 0.1 MPa. The emission spectrum of the meteor indicates that the progenitor meteoroid was chondritic, which is consistent with the results obtained in previous studies. Besides, the analysis of the terminal point of the luminous path revealed that this particle was not completely ablated in the atmosphere. Thus, about 6.5 g survived and fell on the ground. This supports the hypothesis that the Taurids may give rise to meteorite-producing fireballs under favourable conditions. In this case, the landing area was calculated and an expedition was organized to try to recover the surviving mass, but no meteorites were found.

ACKNOWLEDGEMENTS

The author is very grateful to Fundación AstroHita for its support in the establishment and operation of the automated meteor-observing station located at La Hita Astronomical Observatory. In addition, financial support from grant PID2024-161944NB-I00 funded by MCIN/AEI/10.13039/501100011033/, and from the Severo Ochoa grant CEX2021-001131-S funded by MCIN/AEI/10.13039/501100011033 is also acknowledged.

DATA AVAILABILITY

The data underlying this article will be shared on reasonable request to the corresponding author.

REFERENCES

Asher D. J., 1991, The Taurid Meteoroid Complex. PhD Thesis, Oxford University
Asher D. J., Clube S. V. M., Steel D. I., 1993, MNRAS, 264, 93
Babadzhanov P. B., Kokhirova G. I., 2009, A&A, 495, 353
Babadzhanov P. B., Obrubov I. V., 1992, Celest. Mech. Dyn. Astron., 54, 111
Borovička J., Koten P., Spurný P., Boček J., Štork R., 2005, Icarus, 174, 15
Bronshten V. A., 1981, The Physics of Meteoritic Phenomena. Geophysics and Astrophysics Monographs. Reidel, Dordrecht
Brown P., Marchenko V., Moser D. E., Weryk R., Cooke W., 2013, Meteorit. Planet. Sci., 48, 270
Ceplecha Z., 1987, Bull. Astron. Inst. Cz., 38, 222
Ceplecha Z., 1988, Bull. Astron. Inst. Cz., 39, 221
Ceplecha Z., McCrosky R. E., 1976, J. Geophys. Res., 81, 6257
Ceplecha Z., Novakova-Jezkova M., Porubcan V., Kirsten T., Kiko J., Bocek J., 1983, Bull. Astron. Inst. Cz., 34, 195
Ceplecha Z., Borovička J., Elford W. G., ReVelle D. O., Hawkes R. L., 1998, Space Sci. Rev., 84, 327
Clube V., Napier W., 1982, The Cosmic Serpent – A Catastrophist View of Earth History. Faber and Faber, London, UK
Devillepoix H. A. R., 2019, Planet. Sci. J., 2, 223
Haack H., Grau T., Bischoff A., Horstmann M., Wasson J., 2012, Meteorit. Planet. Sci., 47, 30
Jenniskens P., 2006, Meteor Showers and their Parent Comets. Cambridge Univ. Press, Cambridge
Jenniskens P., 2023, Atlas of Earth's Meteor Showers. Elsevier, Amsterdam, p. 824
Jenniskens P., Devillepoix H. A. R., 2025, Meteorit. Planet. Sci., 60, 928
Jenniskens P., Fries M. D., Yin Q.-Z., Zolensky M., Krot A. N., 2012, Science, 338, 1583
Jenniskens P., Nénon Q., Albers J., Gural P. S., Haberman B., 2016, Icarus, 266, 331
Konovalova N. A., 2003, A&A, 404, 1145
Lindblad B. A., 1971a, Smithsonian Contrib. Astrophys., 12, 1
Lindblad B. A., 1971b, Smithsonian Contrib. Astrophys., 12, 14
Madiedo J. M., 2014, Earth Planets Space, 66, 70.
Madiedo J. M., 2015a, Planet. Space Sci., 118, 90
Madiedo J. M., 2015b, MNRAS, 448, 2135

Madiedo J. M., 2017, Planet. Space Sci., 143, 238
Madiedo J. M., 2021, eMeteorNews, 6, 397
Madiedo J. M., Trigo-Rodríguez J. M., Castro-Tirado A. J., Ortiz J. L., Cabrera-Caño J., 2013, MNRAS, 436, 2818
Madiedo J. M., Ortiz J. L., Trigo-Rodríguez J. M., Dergham J., Castro-Tirado A. J., 2014, Icarus, 231, 356
Matlovič P., Tóth J., Rudawska R., Kornoš L., 2017, Planet. Space Sci., 143, 104
Moore C. E., 1945, A Multiplet Table of Astrophysical Interest. Princeton University Observatory, Princeton, NJ. Contribution No. 20.
Southworth R. B., Hawkins G. S., 1963, Smithsonian Contrib. Astrophys., 7, 261.
Spurný P., Borovička J., Mucke H., Svoreň J., 2017, A&A, 605, A68
Steel D. I., Asher D. J., 1996, MNRAS, 281, 937
Steel D. I., Asher D. J., Clube S. V. M., 1991, MNRAS, 251, 632
U.S. Standard Atmosphere, 1976, NOA-NASA-USAF, Washington
Wetherill G. W., 1974, Annu. Rev. Earth Planet. Sci., 2, 303
Whipple F. L., 1940, Proc. Am. Phil. Soc., 83, 711

This paper has been typeset from a TEX/LATEX file prepared by the author.